EFFECTS OF CARBONIZATION TEMPERATURE ON CHEMICAL AND MICROCRYSTALLINE STRUCTURAL CHANGE IN WOOD–CERAMICS PREPARED FROM LIQUEFIED PINE WOOD AND WOOD POWDER

Delin Sun†*

Professor
E-mail: sdlszy@163.com

Xiaofeng Hao

Research Assistant
E-mail: hxf8271@163.com

Xinyi Chen

Research Assistant
College of Material and Engineering
Central South University of Forestry and Technology
Changsha 410004, Hunan, China
E-mail: Chen_xinyi_csuft@126.com

Xiaoxi Huang

Assistant Professor
Biotechnology Core Facilities
Central South University of Forestry and Technology
ChangSha 410004, Hunan, China
E-mail: huangxiaoxi1999@163.com

(Received September 2014)

Abstract. A new type of wood–ceramics was prepared by carbonizing liquefied wood instead of using thermosetting resin. In this study, the effects of the unit cell of the wood powder and the aromatic ring in liquefied wood on the chemical and microcrystalline structural changes of wood–ceramics under different carbonization temperatures were discussed. Results from Fourier transform IR spectroscopy showed that carbonization affected the structure change of functional groups; broke C–H, C–O, and C=C bonds; and facilitated the removal of H^+ and O^{2-}. X-ray diffraction analysis indicated that the microcrystalline structure of both wood and liquefied wood was changed to produce graphene sheets as the carbonization temperature increased, and a higher carbonization temperature contributed to a more orderly arrangement of microcrystalline graphite and formed a six-membered carbon ring structure. The number of graphite microcrystals, crystallite size, and the stacking height of the layer plane increased, whereas d_{002} decreased. The values of d_{002}, L_a, and L_c were 0.3740, 3.2572, and 0.5754 nm as the temperature reached 1600°C, respectively. However, the wood–ceramics remained difficult to completely graphitize.

Keywords: Wood–ceramics, liquefied wood, carbonization temperature, microcrystalline structural change.

INTRODUCTION

Wood–ceramics are considered to be a new carbon material that was developed by artificial coupling of native wood. They retain the fine morphology and structure of biological materials and simultaneously exhibit artificial characteristics and functionality (Izuka et al 1999; Zhang et al 2004). They have low mass and high specific strength, good frictional and thermal characteristics, and excellent electromagnetic properties (Treusch et al 2004; Ozao et al 2005). Therefore, the intended applications include

* Corresponding author
† SWST member

heat-insulating materials, electromagnetic materials, absorbents, catalyst carrier materials, etc. Wood–ceramics were traditionally prepared through high-temperature carbonization of wood impregnated with thermosetting resins, such as phenolic, epoxy, and furan resins. Numerous studies have explored the mechanical properties (Xie and Fan 2002; Zhou et al 2010), friction performance, and conductivity (Yu et al 2012; Kwon et al 2013) of wood–ceramics prepared from medium-density fiberboard and wood powder impregnated with phenol formaldehyde resin (PF). Effects of processing parameters (eg carbonization temperature and heating rate) on the structural changes have also been discussed (Qian et al 2004a).

Despite its extensive use, thermosetting resin presents no significant contribution to sustainable development. Meanwhile, only a few studies have analyzed the microcrystalline structural changes in wood–ceramics during carbonization. Thus, in accordance with Hirose et al (2002) and a previous study (Sun et al 2013), liquefied pine products instead of thermosetting resin were used to prepare wood–ceramics in this study to save resources and protect the environment. The structural transformation of the unit cell of wood and the aromatic ring of liquefied wood into graphite microcrystals was analyzed by Fourier transform IR spectroscopy (FTIR) and X-ray diffraction (XRD): the evolution mechanism of the microcrystalline structure in wood–ceramics during carbonization was explored.

MATERIALS AND METHODS

Preparation Method

Discarded pine brush was powdered with a pulverizer until passing 40 mesh and was then dried to constant mass at 100°C. The pine powder, phenol, and distilled water (mass ratio = 1:3:0.5) were subsequently placed into a four-necked flask. A concentrated sulphuric acid equivalent to 5% (mass ratio) of the pine powder was added as a catalyst. The mixture was reacted for 3 h at 160°C to obtain resinous liquefied wood.

The liquefied wood and pine powder (mass ratio = 1:3) were evenly mixed and dried at 50°C until reaching 8% MC. The mixture was poured into a mold, hot-pressed at 6 MPa and 140°C for 8 min, and then cooled at room temperature. The resulting liquefied wood–powder composite specimen was placed into a carbonization oven (CV-73; Steyr Thermal Technology Co., Ltd., Yixing, China) and was carbonized under the protection of nitrogen at ordinary pressure. The temperature was increased at a rate of 5°C/min to 120°C, which was maintained for 30 min, and thereafter increased at 2°C/min to the desired temperature (eg 600, 1200, or 1600°C) and maintained for 1 h. Finally, the specimen was cooled to ambient temperature in the furnace, and liquefied pinewood-based wood–ceramics were obtained.

Test and Characterization

FTIR (Nicolet 380; Thermo Scientific, Madison, WI) was performed to analyze the changes in functional groups using a KBr pellet technique. Wood–ceramic powder of 1-2 mg was mixed with 200 mg KBr, and a pellet was formed by pressing. The operation parameters were Happ-Genzel apodization, 30 scans, 4.0 cm^{-1} spectral resolution, and 500-4000 cm^{-1} scan range.

XRD (XD-2; Beijing PERSEE Co., Ltd., Beijing, China) was conducted to detect phase changes and the degree of graphitization. The measurement conditions were 50-kV tube voltage, 80-mA tube current, and 2°/min scanning rate. The interlayer spacing (d_{002}) and degree of graphitization (g) were calculated using the Bragg equation (Fujimoto 2003), and the crystallite size (L_a) and stacking height of each layer plane (L_c) were calculated using the Scherrer equation (Aso et al 2004).

RESULTS AND DISCUSSION

The crystal structure of the wood cell wall includes the amorphous region and crystalline region. The Meyer–Misch model (Pizzi and Eaton 1985; Maurer and Fengel 1992) shows

that the unit cells of wood in the crystalline region are parallel and determines the basic characteristics of its crystals. After liquefaction, wood powder turns into a resinous sticky substance that has many aromatic rings and a basic structure similar to PF resin (Ma et al 2011). During carbonization, the degree of polymerization of wood powder decreases and amorphous and crystalline regions are damaged. Structural changes in the aromatic rings also occur in liquefied wood (Nishimiya et al 1998; Ishimaru et al 2007).

Basic Characteristics

Fourier transform IR spectroscopy analysis. The variations in the functional groups during carbonization were detected by FTIR spectroscopy. Figure 1 shows the FTIR patterns of wood–ceramics carbonized at 500°C, pine wood powder, and liquefied wood. The absorption and shoulder peaks at 2850 and 2820 cm^{-1} were the asymmetrical and symmetrical C–H stretching vibrational peaks of aromatics and aliphatics, respectively; these peaks were not observed in the corresponding patterns for wood–ceramics. This indicates that carbonization breaks C–H bonds (Jiang et al 2005), removes some H^+, destroys the unit cells, and excludes both free and bound water. The characteristic peaks at 1600, 1585, 1500, and 1450 cm^{-1} represent the vibrations of the benzene ring, in which the highest intensity is found in the spectrum of liquefied wood because of the free phenol content. Nevertheless, these characteristics significantly weakened and even disappeared in the corresponding patterns for wood–ceramics, denoting that the C=C bonds in any aromatic ring structures have been changed during carbonization. Also, the C–O absorption peaks at 1740 and 1710 cm^{-1} and the C–O–C characteristic absorption peaks at 1250, 950, and 800-900 cm^{-1} almost disappeared in the spectra of wood–ceramics, indicating that the C–O bonds were broken (Nishimiya et al 1998; Dubois et al 2000). Interestingly, the C–H out-of-plane vibrational peak from the aromatic ring vibration near 620 cm^{-1} was still observed in wood–ceramics; this implies that wood–ceramics contain numerous multinuclear hydrocarbon structures at 500°C (Ercin and Yürüm 2003).

The FTIR spectra of wood–ceramics carbonized at 600, 1200, and 1400°C are shown in Fig 2. When the carbonization temperature increased, the absorption peak at 3500 cm^{-1} gradually decreased because of dehydration. However, the C–C in-plane stretching vibration of the aromatic ring at 1450 cm^{-1} presents a decreasing trend, which may have been caused by the rearrangement of C–C bonds during heating. At the same

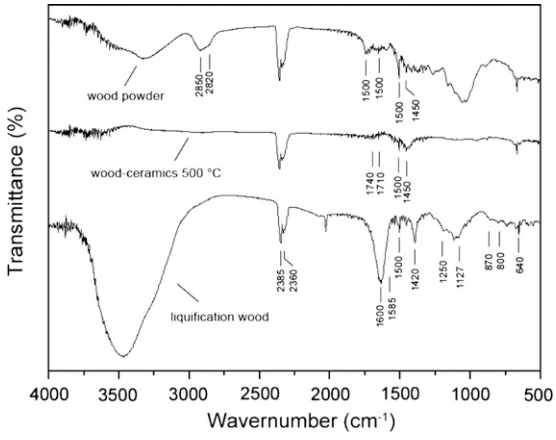

Figure 1. Fourier transform IR spectroscopy patterns of wood powder, liquefied wood, and wood–ceramics.

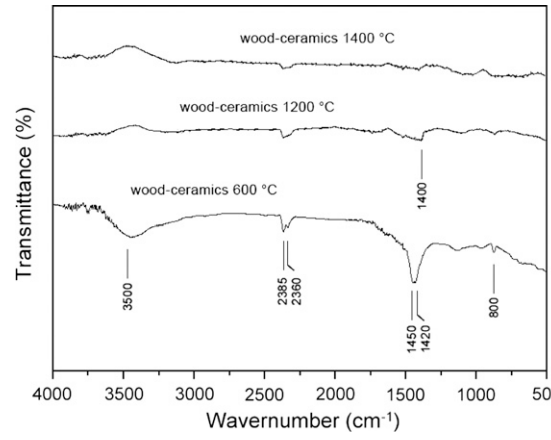

Figure 2. Fourier transform IR spectroscopy patterns of wood–ceramics with different carbonation temperatures.

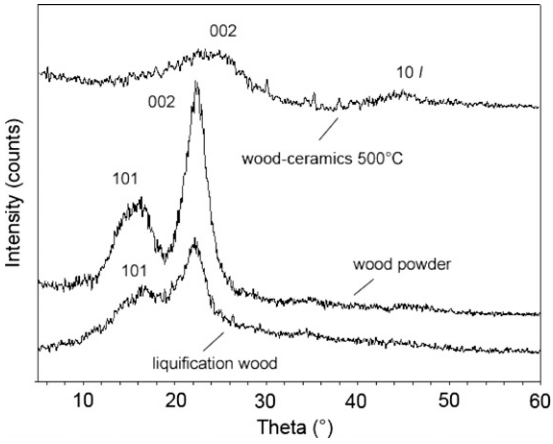

Figure 3. X-ray diffraction patterns of wood powder, liquefied wood, and wood–ceramics.

time, the C–H vibrational peak of the aromatic ring near 800 cm^{-1} also weakened in the sample processed at 1400°C. This phenomenon demonstrates that high temperature can facilitate the removal of H^+ in wood–ceramics.

X-ray diffraction characterization. The microcrystalline structural changes in wood–ceramics during carbonization can be described by the variation in the observed diffraction peaks. The XRD patterns of wood–ceramics, wood powder, and liquefied wood are shown in Fig 3. Wood powder had two obvious diffraction peaks near 16.2° and 22.1° (101 and 002 peaks). They are the special peaks that characterize the amorphous and crystalline regions of wood. In the pattern of liquefied wood, the 101 peak broadened and the height of the 002 peak decreased. However, the XRD pattern of wood–ceramics shows no 101 peak and exhibits a new 10*l* peak near 42°; meanwhile, the 002 peak shifted to a larger angle close to 23°. This condition confirms that during carbonization, the microcrystalline structure of both wood and liquefied wood changed and new microcrystalline structures were formed.

Crystallinity reflects the degree of crystallization during the aggregation of a microcrystal to a certain extent. The relative crystallinities of wood powder, liquefied wood, and wood–ceramics are listed in Table 1 (based on Fig 3). The relative crystallinities of wood powder and liquefied wood (residue not filtered) were 61.48 and 47.72%, respectively. A 10*l* diffraction peak appeared in the sample carbonized at 500°C, and the 002 peak became larger in the sample carbonized at 1400°C with corresponding crystallinities of 30.12 and 44.03%; this indicates that the relative crystallinity increased (ie improved) when its carbonization temperature increased.

Structural Evolution Mechanism

With different carbonization conditions, the unit cells of wood and the aromatic ring of liquefied wood changed. This was mainly caused by pyrolysis-induced behavior at low temperature and restructuring and graphitization at high temperature (Nishimiya et al 1998).

Microcrystalline structural changes in wood carbonized at low temperature. Based on Figs 1-3 and according to previous studies (Shafizadeh 1975; Shafizadeh and Chin Peter 1977), the woody materials carbonization process can be described with the following stages:

(a) First stage (25-150°C): desorption of absorbed water in the wood and discharge of free water;

Table 1. Relative crystallinity of wood powder, liquefied wood, and wood–ceramics.

	Parameter						
	101 peak		002 peak		10*l* peak		
Materials	2θ (°)	Height (cps*)	2θ (°)	Height (cps)	2θ (°)	Height (cps)	Relative crystallinity (%)
Wood powder	16.23	203	22.14	527	—	—	61.48
Liquefied wood (residue no filtered)	16.42	106	22.23	241	—	—	56.02
Wood–ceramics (500°C)	—	—	21.32	83	42.67	58	30.12
Wood–ceramics (1400°C)	—	—	22.97	109	43.21	61	44.03

* cps is count rate (counts per second).

(b) Second stage (150-240°C): dehydration (bound water) of the glucosyl group in wood and decrease in cellulose intensity;
(c) Third stage (240-400°C): damaging of amorphous and crystalline regions in the wood as well as damaging the unit cell, breakage of glucosidic bonds, production of micromolecules (eg H_2O, CO, and CO_2), 1,6-Anhydro-β-D-glucopyranose, and wood tar at temperatures greater than 300°C; and
(d) Fourth stage (>400°C): beginning of aromatic cyclization of residual carbons as well as rearrangement of unit cells and conversion to the graphite crystal structure.

Changes in aromatic rings of liquefied wood carbonized at low temperature. Figure 4 shows the sketch map of the pyrolysis and structural changes of liquefied wood. During the early stage of carbonization at low temperature, the liquefied wood is polycondensed, dehydrated (I and II), and solidified to form a methylene bridge (Zhang et al 2006; Huang et al 2012). Pyrolysis begins after the carbonization temperature increases to approximately 200°C. During this period, two phenolic groups react and produce ether bonds (III) and water. Meanwhile, the phenolic groups are polycondensed with the methylene bridge to produce diphenylmethane structures (IV). After the carbonization temperature exceeds 400°C, the liquefied wood is polycondensed and cyclized, producing diphenyl-pyran ring structures (V). Finally, the liquefied wood is further carbonized and dehydrogenated into glassy carbon.

Microcrystalline structural changes in wood–ceramics carbonized at high temperature. At higher temperatures (>400°C), H^+ and O^{2-} remained in the residual carbon of wood powder and the glassy carbon of liquefied wood was further removed; this was accompanied by the aforementioned structural rearrangement (Qian et al 2004a; Kumagai and Sasaki 2009). The XRD pattern of wood–ceramics prepared under high-temperature carbonization is shown in Fig 5, and the corresponding parameters are listed in Table 2. The values of d_{002} decreased with increasing carbonization temperature: they decreased from 0.4015 to 0.3740 nm when the temperature increased from 700 to 1600°C and approached 0.3354 nm (one value of the interlamellar spacing of an ideal graphite crystallite), demonstrating that wood–ceramics have a tendency to transform into graphite structures with increasing carbonization temperature (Cheng et al 1999). This is because the increase of carbonization temperature could increase the amount of graphite crystallite, the coherent length, and the crystallite layer thickness, which results in more uniform arrangements of the hexagonal network crystallite layers (Ma et al 2014). However, d_{002} is always larger than 0.3354 nm, which confirms

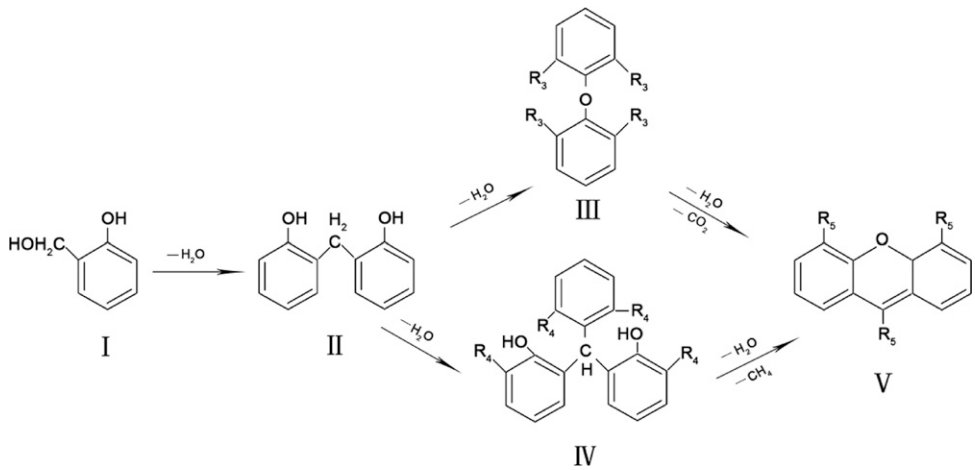

Figure 4. Carbonization process of liquefied wood at low temperature.

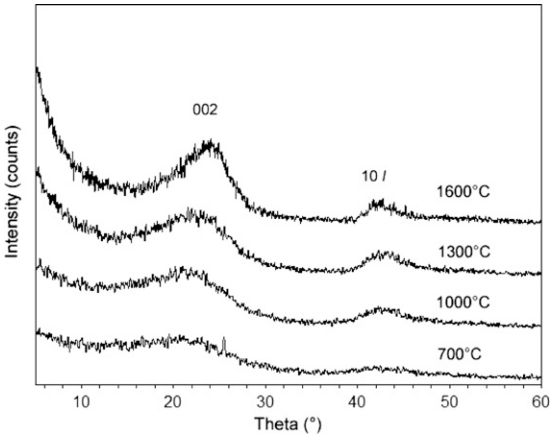

Figure 5. X-ray diffraction patterns of wood–ceramics carbonized at high temperature.

that wood–ceramics prepared under the conditions used in this study are difficult to graphitize but their structures become more regular and orderly with increasing carbonization temperature. The results agree with those obtained by Qian et al (2004b) who prepared wood–ceramics from phenolic resin–basswood powder.

Table 2 also shows that L_c/d_{002} values were less than 1 at 700°C, which indicates that the single-layer graphene sheets were incomplete. As the temperature increased to 1000°C, L_c/d_{002} increased to a value greater than 1, denoting the existence of one layer of graphite microcrystals. That is because when the carbonization temperature increased, H^+ and O^{2-} were gradually removed and the carbon ring structures and the plane of the carbon network became more orderly. Meanwhile, the graphene sheet further shrank, and a microcrystalline structure of stacked graphene sheets was formed. Also, the diameter of the microcrystal and the number and layers of graphene sheets continuously increased. When L_a increased, sp^2 hybridization carbon in the corresponding graphene sheets increased accordingly and the number of edge carbon atoms in the graphene sheets and sp^3 hybridization carbon in the incompletely pyrolyzed disorderly tetrahedron network decreased (Zhou et al 2005). Therefore, higher carbonization temperatures are beneficial with regard to improving the microstructure of wood–ceramics.

The microcrystalline structural change of wood–ceramics under high temperature is shown in Fig 6. The residual carbon in wood began to be aromatized at approximately 400-700°C. During aromatization, the carbon residuals produced in the elimination reaction of pyran rings with other intermediate products of carbonization condensed and the unit cells were rearranged to form a lamellar structure. Meanwhile, the diphenyl-pyran ring structure formed by liquefied wood was dehydrogenated. After the carbonization temperature exceeded 700°C, elemental H and O were further removed, forming carbon ring structures and transforming into a lamellar graphite microcrystalline structure.

The d_{002} values of the specimen were greater than 0.3354 nm in Table 2, although the carbonization temperature reached 1600°C. This result also confirms that wood–ceramics prepared under the experimental conditions used for this study are difficult to graphitize. This phenomenon may have been caused by the fact that the net planes of the six-membered carbon ring gradually expanded and began to individually pile up on each other, forming a parallel arrangement and then forming graphite microcrystals during carbonization. However, carbon atoms were connected by covalent bonds in the net planes, whereas between the net planes, they were connected by intermolecular forces, which

Table 2. Parameters of X-ray diffraction for wood–ceramics carbonized under different temperature.

Temperature (°C)	$2\theta_{(002)}$ (°)	d_{002} (nm)	$2\theta_{(10l)}$ (°)	d_{10l} (nm)	$g_{(002)}$	L_a (nm)	L_c (nm)	L_c/d_{002}
700	22.12	0.4015	42.723	0.2115	−4.107	2.5314	0.3261	0.8122
1000	22.51	0.3945	42.324	0.2134	−3.607	2.7421	0.4075	1.0330
1300	22.93	0.3875	42.609	0.2099	−3.107	3.0165	0.5754	1.4826
1600	23.78	0.3740	42.730	0.2114	−2.143	3.2572	0.6327	1.6917

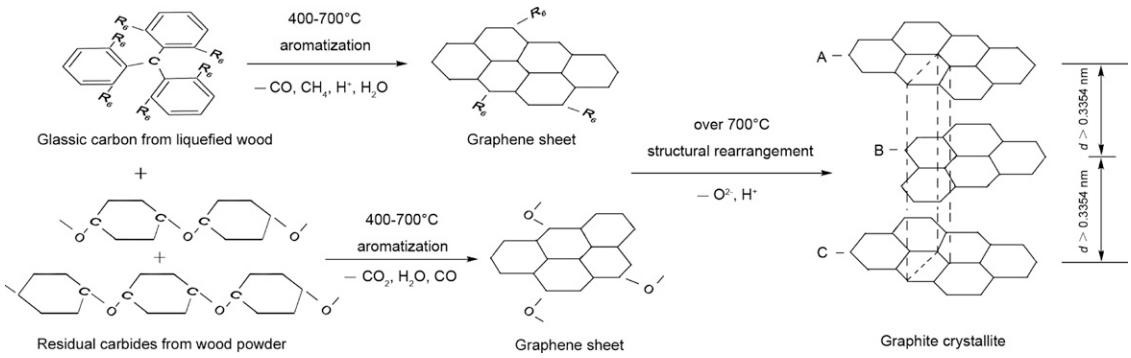

Figure 6. Microcrystalline structural change model of wood–ceramics carbonized at high temperature.

led to the observed anisotropy. Hence, although the graphite crystals were arranged in a more orderly fashion when the carbonization temperature further increased, such an arrangement still remained turbostratic (structure ABC in Fig 6) compared with a parallel arrangement similar to that of the ABAB structure of graphite.

CONCLUSIONS

Wood–ceramics were prepared with pine wood powder and liquefied pine wood instead of impregnation with thermosetting resin, implying a potential to be a replacement of conventional thermosetting resins in the wood–ceramic industry. Carbonization temperature was an important factor that directly affected the interplanar spacing of the ensuing microcrystalline structural changes. During carbonization, the amorphous and crystalline phases of the wood were destroyed, the aromatic ring structure of the liquefied wood was polycondensed, and the relative crystallinity improved when the carbonization temperature increased. The aromatic ring structure of liquefied wood was polycondensed and dehydrated before the temperature reached 400°C. At 400-700°C, the polycondensation and cyclization were accelerated and some residual carbons formed several graphene sheets. At temperatures greater than 700°C, the cumulative thickness of graphene sheets and the diameter of the microcrystalline components increased with increasing carbonization temperature: the H^+ and O^{2-} residuals were further removed. The structure of wood–ceramics was rearranged, and the graphite microcrystalline structure was developed. Nevertheless, the structure remained turbostratic even at 1600°C.

ACKNOWLEDGMENT

We gratefully acknowledge the financial support from the National Natural Science Foundation of China (No. 31270611).

REFERENCES

Aso H, Matsuoka K, Sharma A, Tomita A (2004) Structural analysis of PVC and PFA carbons prepared at 500-1000 °C based on elemental composition, XRD, and HRTEM. Carbon 42(14):2963-2973.

Cheng HM, Endo H, Zheng GB (1999) Graphitization behavior of wood ceramics and bamboo ceramics as determined by X-ray diffraction. J Porous Mater 6(3):233-237.

Dubois M, Naji A, Buisson JP, Humbert B, Grivei E, Billaud D (2000) Characterisation of carbonaceous materials derived from polyparaphenylene pyrolyzed at low temperature. Carbon 38(9):1411-1417.

Ercin D, Yürüm Y (2003) Carbonization of fir (*Abies bornmulleriana*) wood in an open pyrolysis system at 50-300°C. J Anal Appl Pyrol 67(1):11-22.

Fujimoto H (2003) Theoretical X-ray scattering intensity of carbons with turbostratic stacking and AB stacking structures. Carbon 41(8):1585-1592.

Hirose T, Zhao BY, Okabe T, Yoshimura M (2002) Effect of carbonization temperature on the basic properties of woodceramics made from carbonized bamboo fiber and liquefied wood. J Mater Sci 37(16):3453-3458.

Huang N, Liu L, Wang XY (2012) Pyrolysis and kinetics of phenolic resin by TG-MS analysis. Aerospace Materials & Technology l 41(2):99-102.

Ishimaru K, Hata T, Bronsveld P, Nishizawa T, Imamura Y (2007) Characterization of sp^2- and sp^3-bonded carbon in wood charcoal. J Wood Sci 53(5):442-448.

Izuka H, Fushitani M, Okabe T (1999) Mechanical properties of wood–ceramics: A porous carbon material. J Porous Mater 6(3):175-184.

Jiang MS, Huang B, Chen XR, Tang XP (2005) FT-IR spectroscopic analysis on wood carbonization mechanism. Chemistry and Industry of Forest Products 25(2):16-20.

Kumagai S, Sasaki J (2009) Carbon/silica composite fabricated from rice husk by means of binderless hot-pressing. Biores Technol 100(3):3308-3315.

Kwon JH, Park SB, Ayrilmis N, Oh SW, Kim NH (2013) Effect of carbonization temperature on electrical resistivity and physical properties of wood and wood-based composites. Compos, Part B Eng 46(3):102-107.

Ma XJ, Yuan C, Liu XY (2014) Mechanical, microstructure and surface characterizations of carbon fibers prepared from cellulose after liquefying and curing. Materials 7(1):75-84.

Ma XJ, Zhao GJ, Liu XY, Yu LL (2011) Effects of carbonization temperatures on the adsorption properties and pore structure of carbon fibers from liquefied wood. J Functional Materials 42(10):1746-1749.

Maurer A, Fengel D (1992) Parallel orientation of the molecular chains in cellulose I and cellulose II deriving from higher plants. Holz Roh Werkst 50(12):493-498.

Nishimiya K, Hata T, Imamura Y, Ishihara S (1998) Analysis of chemical structure of wood charcoal by X-ray photoelectron spectroscopy. J Wood Sci 44(1):56-61.

Ozao R, Okabe T, Arii T, Nishimoto Y, Cao Y, Whitely N, Pan WP (2005) Gas adsorption properties of woodceramics. Mater Trans 46(12):2673-2678.

Pizzi A, Eaton N (1985) The structure of cellulose by conformational analysis. Part 3. Crystalline and amorphous structure of cellulose I. J Macromol Sci Chem 22(2):139-160.

Qian JM, Jin ZH, Wang JP (2004a) Study on structural changes during preparing woodceramics from corncob and phenolic resin/basswood powder composite. Acta Materiae Compositae Sinica 21(4):18-23.

Qian JM, Jin ZH, Wang JP (2004b) Structure and basic properties of woodceramics made from phenolic resin–basswood powder composite. Mater Sci Eng A 368(1):71-79.

Shafizadeh F (1975) Industrial pyrolysis of cellulosic materials. Appl Polym Symp 28. Pages 153-174 *in* Proc Eighth Cellulose Conference I. Wood Chemicals—A Future Challenge. John Wiley & Sons, Inc., New York, NY.

Shafizadeh F, Chin Peter PS (1977) Thermal deterioration of wood, Wood Technology: Chemical Aspects. Pages 57-81 in IS Goldstein, ed. ACS Sym Series, Vol. 23. ACS, Washington, DC.

Sun DL, Yu XC, Wang R (2013) Characterization of woodceramics prepared from liquefied corncob and poplar powder. Asian J Chem 25(1):373-376.

Treusch O, Hofenauer A, Tröger F, Fromm J, Wegener G (2004) Basic properties of specific wood-based materials carbonized in a nitrogen atmosphere. Wood Sci Technol 38(5):323-333.

Xie XQ, Fan TX (2002) Increasing the mechanical properties of high damping woodceramics by filtration with magnesium alloy. Compos Sci Technol 62(10-11): 1341-1346.

Yu XC, Sun DL, Sun DB, Xu Z, Li XS (2012) Basic properties of woodceramics made from bamboo powder and epoxy resin. Wood Sci Technol 46(1):23-31.

Zhang D, Sun BH, Fan TX (2004) Preparation and micromechanism analyse of Morph-genetic materials. Science in China Series E 34(7):721-729.

Zhang YN, Xu YD, Gao LY, Zhang LT, Chang LF (2006) Microstructural evolution of phenolic resin-based carbon/carbon composites during pyrolysis. Acta Materiae Compositae Sinica 23(1):37-43.

Zhou DF, Xie HM, Zhao YL, Wang RS (2005) Graphitizing degree and electrochemical properties of carbonaceous material by phenolic resin pyrolyzing. J Funct Mater 36(1):83-85.

Zhou WH, Yu YS, Xiong XL (2010) Basic properties of woodceramics made from furane resin/bamboo powder composite. Advanced Materials Research 160-162: 1569-1574.